2-15-2010

Oxygen Regulates The Effective Diffusion Distance of Nitric Oxide in The Aortic Wall

Xiaoping Liu
Ohio State University

Parthasarathy Srinivasan
Cleveland State University, p.srinivasan35@csuohio.edu

Eric Collard
Ohio State University

Paula Grajdeanu
Ohio State University

Kevin Lok
Ohio State University

See next page for additional authors

Authors
Xiaoping Liu, Parthasarathy Srinivasan, Eric Collard, Paula Grajdeanu, Kevin Lok, Sarah E. Boyle, Avner Friedman, and Jay L. Zweier

Original Contribution

Oxygen regulates the effective diffusion distance of nitric oxide in the aortic wall

Xiaoping Liu, Parthasarathy Srinivasan, Eric Collard, Paula Grajdeanu, Kevin Lok, Sarah E. Boyle, Avner Friedman, Jay L. Zweier

Nitric oxide (NO) is a diffusible diatomic molecule. In blood vessels, after NO molecules are generated from endothelial NO synthase (NOS), some NO molecules diffuse into the lumen to react with hemoglobin within red blood cells (RBCs) in the blood. Other NO molecules diffuse into the vascular wall to activate soluble guanylate cyclase (sGC) in smooth muscle cells, initiating a series of events leading to the dilation of the blood vessel. The extent of vasodilation is determined by the effective NO diffusion distance, and the effective NO diffusion distance is regulated by multiple factors in the vascular system.

Computer simulation shows that hemoglobin (Hb) in the luminal blood can significantly alter the NO concentration distribution in the vascular wall and surrounding tissue [1]. This is because the hemoglobin concentration and its distance to the NO source (endothelial cell layer) can largely affect the NO concentration at the endothelial cell layer, whereas the NO concentration distribution in the vascular wall is proportional to the NO concentration at the endothelial cell layer. These theoretical results provided important information for understanding the effects of *luminal* Hb on NO bioavailability in the vascular wall. It is known that the reaction of NO with oxyhemoglobin (oxyHb) is extremely rapid. To understand how endothelium derived NO escapes the vast amount of Hb (~15 g/dl or ~2.3 mM) [2] in the blood and diffuses to the smooth muscle cells to stimulate sGC within these cells, we compared the rate of NO consumption by cell free oxyHb and the oxyHb enclosed in RBCs. It was observed that the rate of the NO reaction with the RBC enclosed Hb is nearly 1000 times slower than that with cell free Hb [3,4], though the explanations for this phenomenon remain controversial [3 9]. In addition to the blood, other factors may also be involved in the regulation of NO concentration in the vascular wall. Studies on NO consumption by mammalian cells demonstrate that cellular NO consumption is oxygen dependent, but the majority of consumption is not caused by the direct reaction between NO and oxygen [10,11]. This is because the measured rate of cellular NO consumption is much greater than the rate of NO autoxidation by oxygen and the kinetic order of cellular NO consumption is different from that of NO autoxidation. Kinetic measurements have shown that the rate of NO consumption by parenchymal cells (hepatocytes) is first order with respect to [O_2] and first order with respect to [NO] [10], whereas NO autoxidation is second order with respect to [NO] [12 14]. Recent evidence has shown that mitochondrial cytochrome *c* oxidase[15] and cytoglobin [16] are involved in the oxygen dependent consumption of NO in cells. However, it is still unknown if the oxygen regulated NO consumption rate in the vascular wall has the same kinetics characteristics as in

isolated cells, and if this oxygen regulated NO consumption rate can significantly affect the NO diffusion distance in the vascular wall. In this study, a recently developed experimental technique, together with related mathematical models, was used to examine how the effective NO diffusion distance changes in the aortic wall at various oxygen concentrations.

Experimental methods

Preparation of NO solution

NO gas was scrubbed of higher nitrogen oxides by passage first through a U tube containing NaOH pellets and then through a 1 M deaerated (bubbled with 100% argon) KOH solution, in a custom designed apparatus constructed of only glass or stainless steel tubing and fittings [10,17]. The purified NO was collected by saturating a deaerated phosphate buffer solution (0.2 M potassium phosphate, pH 7.4) contained in a glass sampling flask with a septum purchased from Kimble/Kontes (Vineland, NJ, USA). NO can react with oxygen to form the toxic products NO_2 and N_2O_4. Therefore, NO solutions were prepared in a fume hood.

Isolation of rat aorta

WKY rats were anesthetized with pentobarbital (100 mg/kg, ip). A segment of thoracic aorta (~3 cm in length) was rapidly dissected and placed into an ice cold phosphate buffer solution with glucose (pH 7.4) of the following composition: 137 mM NaCl, 2.5 mM KCl, 0.9 mM $CaCl_2$, 0.5 mM $MgSO_4$, 1.5 mM KH_2PO_4, 0.8 mM Na_2HPO_4, and 5.6 mM glucose. The blood in the aorta was immediately flushed, and loosely adherent fat and connective tissue were removed. The aorta was equilibrated in the tissue buffer solution at 37°C for 3×20 min. After incubation, two short aortic rings (~2 mm long) were cut from the two ends of the aortic segment. This pair of aortic rings was used to measure the thickness of the aortic wall. Then the remaining segment (~2.6 cm) was cut into two aortic rings of equal length for electrochemical measurements of NO diffusion fluxes. The use of animals and the animal protocol were approved by the Institutional Lab Animal Care and Use Committee of The Ohio State University.

Measurements of thickness of aortic wall and tunica media

The wall of an artery mainly consists of layers: the tunica intima (TI), the tunica media (TM), and the tunica adventitia (TA). The TI is the innermost layer of the artery wall and comprises an endothelial cell monolayer (endothelium) supported by connective tissue. The TM is the middle, and thickest, layer of the wall and contains smooth muscle cells embedded in an extracellular matrix composed mainly of collagen, elastin, and proteoglycans. The TA is the outer layer of the wall, consisting of mostly collagen. Because the TI is much thinner than the TM, the thickness of the TM is approximately equal to the total thickness of TI and TM. A hematoxylin and eosin (H&E) stained aortic section is shown in Fig. 1 (H&E staining is a popular staining method in histology). To measure the wall thicknesses of an aortic ring, the aortic ring was placed under a precision stereo zoom trinocular microscope (World Precision Instruments, Sarasota, FL, USA) equipped with a color video camera. The wall thicknesses at five locations on the cross section of each ring were measured. A value of the final wall thickness of the aorta was obtained by the average of 10 readings from the pair of aortic rings. To estimate the thickness of the TM, we first measured the thickness of the TM (l_{TM}) and the thickness of the aortic wall (l_a) and then computed their ratio at various locations in the image. The average ratio was multiplied by the average thickness of the aortic wall (L) to obtain the average thickness of the TM. In our experiments, L is around 140 μm, and the average ratio is 0.8 with a standard error of ±0.04, so the average thickness of the TM, L_{TM}, is 112 ± 6 μm.

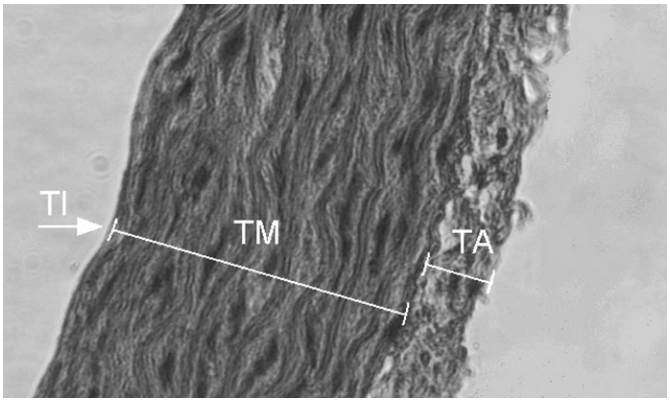

Fig. 1. A section of aorta with H&E staining. TI, tunica intima; TM, tunica media; and TA, tunica adventitia.

Electrochemical measurements of NO diffusion fluxes across the aortic wall at various oxygen concentrations

The experimental setup for measuring the NO diffusion across the aortic wall at various oxygen concentrations was similar to that described previously [18]. A water jacketed chamber contained 15 ml tissue buffer at 37°C. The solution was stirred by a magnetic bar on a stirrer. The chamber was sealed by a cap. One O_2 electrode was used to monitor [O_2] in the solution. After the NO electrodes were stabilized, an O_2/N_2 gas mixture (containing 20, 15, 10, or 5% O_2) was bubbled into the solution through a gas inlet tube for at least 15 min. After [O_2] reached equilibrium, the gas inlet tube was taken out from the solution and remained above the solution surface. NO (3 μM) was injected into the chamber to measure the ratio of NO concentration to the current recorded at the measure ment electrode. Then an aortic ring was longitudinally opened and placed flat on the measurement electrode with the endothelium facing the solution. NO (3 μM) was injected into the chamber. NO diffuses across the aortic wall from the endothelial surface to the adventitial surface. The NO diffusion flux out of the adventitial surface, referred as "NO diffusion flux" in the following text, was recorded by the measurement electrode and [NO] in the solution was recorded by a monitor electrode. After the diffusion fluxes reached their plateau, the O_2/N_2 gas mixture was inserted into the solution again to quickly bring the remaining NO out of the solu tion. The measurement was repeated three times at each oxygen concentration.

The mathematical model for determining rate constants of NO consumption in the aortic wall

It has been reported previously that the consumption rate of NO by cells is first order with respect to [NO] and first order with respect to [O_2] [10]. We assume that NO consumption in the aortic wall has the same kinetic order. Because NO concentration in the solution is nearly a constant during the measurements of NO diffusion flux and the aortic wall is placed flat on the electrode, NO diffusion across the aortic wall on the Clark type NO electrode can be described by the equations

$$D\frac{d^2[\mathrm{NO}]}{dx^2} - k_1[\mathrm{O_2}][\mathrm{NO}] = 0, \tag{1}$$

$$D_{\mathrm{O2}}\frac{d^2[\mathrm{O_2}]}{dx^2} - q = 0, \tag{2}$$

$$[NO] = c_s \text{ at } x = 0, \tag{3}$$

$$[O_2] = u_s \text{ at } x = 0, \tag{4}$$

$$[NO] = 0 \quad \text{at} \quad x = L, \tag{5}$$

$$\frac{d[O_2]}{dx} = 0 \quad \text{at} \quad x = L, \tag{6}$$

where D and D_{O2} are the NO and oxygen diffusion coefficients in the aortic wall, respectively; L is the thickness of the aortic wall; k_1 is the second order rate constant of NO consumption by vascular heme proteins; q is the oxygen consumption rate in the aortic wall, and c_s and u_s are the NO and oxygen concentrations in the solution ($x = L$), respectively. As the effect of the NO autoxidation term in the aortic wall in Eq. (1) and the Michaelis Menten oxygen consumption in Eq. (2) are small, we have ignored these terms in the data analysis. The Clark type NO electrodes were connected to a Free Radical Analyzer 4000 (World Precision Instruments). For detecting NO, the instrument applies a positive potential on the electrode to oxidize all NO that reaches the electrode surface ($x = L$). In our experiments, tissue surrounding the aorta was removed. The oxygen consumption rate in the arterial wall is relatively low, between 1.1×10^{-3} and 4.5×10^{-3} ml/min/g [19], or 0.75 3.4 μM/s. We have previously reported that a segment of 4 cm long aorta consumes 200 μM O_2 in 2 ml buffer solution in 60 min [20]. The volume of this segment is ~50 μl. It can be calculated that the rate of oxygen consumption in the rat aortic wall is ~2 μM/s. This number is within the range given above and also close to the value used in the literature [21,22]. Using this oxygen consumption rate, we simulated the oxygen concentration profile in the aortic wall. It was observed that the average $[O_2]$, $\bar{u}$, in the aortic wall is 2 and 9% lower than u_s ($[O_2]$ in the solution) at $u_s = 200$ μM and $u_s = 50$ μM, respectively. Although the differences between $\bar{u}$ and u_s are small, for more accuracy, we still consider the effect of the distribution of the oxygen concentration on the NO concentration profile in the aortic wall in the above diffusion reaction problem (Eqs. (1) (6)).

The mathematical model for simulations of NO concentration distribution in the aortic wall

When NO and O_2 diffuse through vascular walls, there is an inter action between the two gas molecules in addition to their consump tion in the vascular wall. After the rate constants of their diffusion and reaction kinetics are known, it is possible to use mathematical models to describe the diffusion, reaction, and interaction of the two gas molecules and simulate the NO concentration profile in the vascular wall in different environments. The following mathematical model was used to simulate the NO concentration profile in the aortic wall assuming that the NO and oxygen concentrations at the endothelium are c_e and u_e and the adventitia (TA) faces the buffer solution in vitro:

$$D\frac{d^2[NO]}{dx^2} - k_1[O_2][NO] - k_2[O_2][NO]^2 = 0, \tag{7}$$

$$D_{O2}\frac{d^2[O_2]}{dx^2} - \frac{V_{max}[O_2]}{[O_2] + K_{max}(1 + [NO]/k_{NO})} - \frac{1}{4}k_2[O_2][NO]^2 = 0, \tag{8}$$

$$[NO] = c_e \quad \text{at } x = 0, \tag{9}$$

$$[NO] = 0 \quad \text{at } x \to \infty, \tag{10}$$

$$[O_2] = u_e \quad \text{at } x = 0, \tag{11}$$

$$\frac{d[O_2]}{dx} = 0 \quad \text{at } x \to \infty \tag{12}$$

where D, D_{O2}, and k_1 have the same meaning as in Eqs. (1) (6); k_2 is the third order rate constant of NO autoxidation; and V_{max}, K_{max}, and k_{NO} are the maximum O_2 consumption rate, Michaelis Menten constant for O_2, and inhibition constant for NO in the aortic wall, respectively. We let $V_{max} = 2$ μM/s in the aortic wall and 0 in the surrounding solution, $K_{max} = 1.34$ μM and $k_{NO} = 27$ nM [21], and $k_2 = 1.2 \times 10^7$ M^{-2} s^{-1} [23]. The endothelial surface is assumed at $x = 0$, and the TM and TA are located at the range of $x > 0$. From the literature, the NO concentration at the endothelial surface, c_e, was assumed between ~0.1 and 1.3 μM [1,21,24,25]. In our simulations, we let $c_e = 0.1$ and 1 μM. To observe the effect of oxygen on the vascular NO concentration profile, we can solve Eqs. (7) (12) at various u_e numerically.

Results

Measurements of NO diffusion flux across the aortic wall at various oxygen concentrations

To observe the effects of $[O_2]$ on NO diffusion flux across the aortic wall, we measured the NO diffusion flux at various oxygen concentrations. After 3 μM NO was injected into the chamber, NO diffused from the solution into the aortic wall. The NO diffusion across the aortic wall was measured by a Clark type NO electrode, whereas NO concentration in the solution was monitored by another NO electrode. It was observed that the decay rate of NO in the solution has very small dependence on O_2 concentration in the chamber when NO concentrations are in the low micromolar range (Fig. 2A). In contrast, the NO diffusion flux across the aortic wall significantly increases by

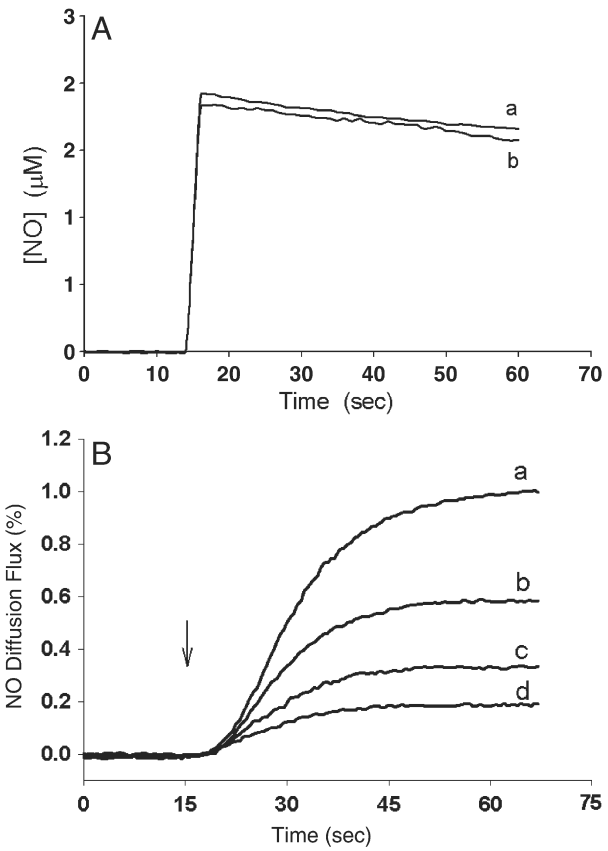

Fig. 2. Measurements of NO diffusion flux across the aortic wall and NO concentration in the solution at various oxygen concentrations. (A) NO concentration in the solution at (curve a) $[O_2] = 0$ μM and (curve b) $[O_2] = 150$ μM. (B) NO diffusion flux across the aortic wall in the presence of (curve a) 0 μM, (curve b) 50 μM, (curve c) 100 μM, and (curve d) 150 μM O_2. The arrow indicates the NO injection time.

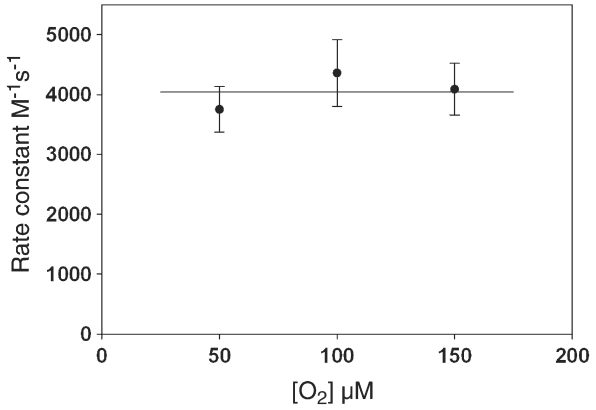

Fig. 3. Measurements of the rate constant for vascular NO consumption. The rate constants determined from experimental data at three oxygen concentrations (50, 100, and 150 μM) are similar. The mean and standard error of the rate constants is $k_1 = (4.0 \pm 0.3) \times 10^3$ M $^{-1}$ s $^{-1}$ ($n = 6$).

around fivefold when the oxygen concentration decreases from 150 to 0 μM (Fig. 2B).

Rate constant of NO consumption in the aortic wall

The rate constants of NO consumption in the aortic wall were determined from the relative NO diffusion flux using Eqs. (1) (6). Because the aortic wall thickness L could be measured under a microscope, and D, D_{O2}, q, c_s, and u_s in the aortic wall were known, we could determine k_1 from the experimental data at a given $[O_2]$ numerically. The determined rate constants at various $[O_2]$ are presented in Fig. 3. The average rate constant $k_1 = (4.0 \pm 0.3) \times 10^3$ M^{-1} s^{-1} ($n = 6$).

Computer simulation of NO concentration distribution in the aortic wall

NO concentration distribution in the aortic wall at various oxygen concentrations can be simulated using Eqs. (7) (12). In the simulation, we assumed that $D = 850$ μm^2/s [18], $k_1 = 4.0 \times 10^3$ M^{-1} s^{-1} and 0 in the aortic wall and in the surrounding solution respectively, and $c_e = 1$ or 0.1 μM. Other parameters can be found in the descriptions of mathematical models under Experimental methods. The simulated results are shown in Figs. 4A and 4B. NO concentrations decrease with distance from the endothelial surface and drop more rapidly as oxygen concentration increases. To connect NO concentration distribution with physiological function of vasorelaxation, we adopted the concept of the effective NO diffusion distance that has been previously introduced in the literature [24]. The effective NO diffusion distance is the distance from the endothelium within which NO concentration is greater than a characteristic NO concentration in the vascular wall. In this study, the characteristic NO concentration (EC_{1ma}) is defined as the NO concentration at the interface between the TM and the TA in the aortic wall when NO concentration at the endothelial surface is 1 μM and oxygen concentration u_e is 200 μM (equilibrium with room air) (Fig. 4). In Fig. 4A, the NO concentration at the endothelial surface is 1 μM, and it decreases to 0.034 μM at the distance of 112 μm from the endothelial surface when $u_e = 200$ μM, so that $EC_{1ma} = 0.034$ μM. Using this EC_{1ma}, we determined the effective NO diffusion distance (d_e) in the aortic wall. To compare among aortas with different wall thicknesses, we define the relative effective diffusion distance (d_r) as

$$d_r = \frac{d_e}{L_{TM}}. \tag{13}$$

The relationship between d_r and the various oxygen concentrations is presented in Fig. 5.

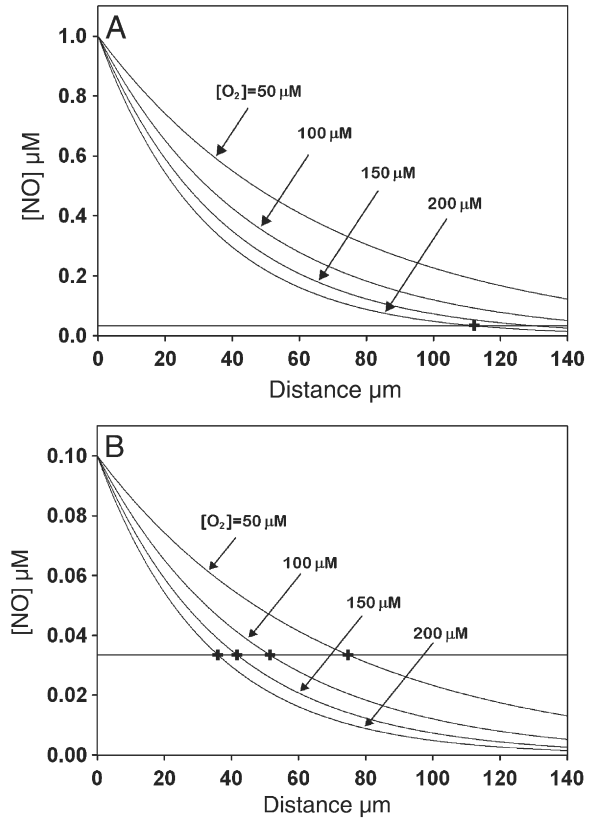

Fig. 4. Simulations of NO concentration in the aortic wall at various oxygen concentrations ($[O_2] = 50$, 100, 150, and 200 μM). (A) Simulation assuming that NO concentration at the endothelial surface is 1 μM. (B) Simulation assuming that NO concentration at the endothelial surface is 0.1 μM. The NO concentration at 80% of the wall thickness ($L_{TM} = 112$ μm), EC_{1ma}, is used to determine the effective NO diffusion distance.

Discussion

Our experimental data demonstrate that the flux of NO diffusion across the aortic wall is oxygen dependent (Fig. 2). Based on these experimental data, we used the mathematical model represented by Eqs. (1) (6) to determine the NO reaction rate constants in the aortic wall. In the mathematical model, we assumed that the rate of NO consumption in the aortic wall follows second order kinetics, first order with respect to [NO] and first order with respect to $[O_2]$, as

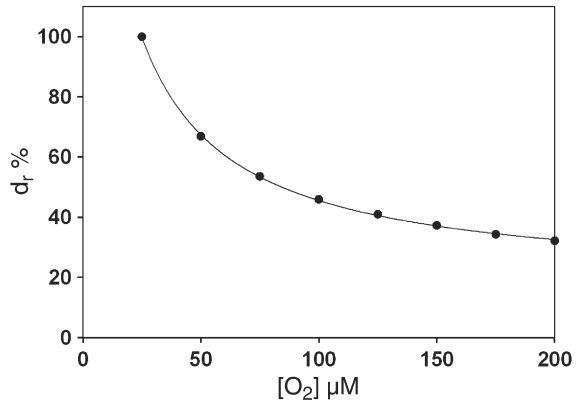

Fig. 5. Change in relative effective NO diffusion distance with oxygen concentration when NO concentration at the endothelial surface is 0.1 μM.

observed in cells [10,11]. The NO consumption rate constants determined at various O_2 concentrations do not significantly vary (Fig. 3), indicating that this second order kinetic model is suitable for modeling the NO biotransport process in the vascular wall at various oxygen concentrations.

After the kinetic parameters were determined from the experimental data, we simulated NO concentration distribution curves in the aortic wall. In this way, we can directly examine how oxygen concentration changes NO concentration distribution in the vascular wall. To bridge the relationship between the vascular NO concentration distribution with the general physiological function of blood vessels, the concept of effective NO diffusion distance based on a characteristic NO concentration [24], EC_{1ma}, is used to represent NO bioavailability in the vascular wall. The characteristic NO concentration is directly related to the vasorelaxation response to NO. It has been shown that aortic rings reach 100% vasorelaxation in the presence of 10 μM NO, and 1 μM NO can induce more than 90% of the vasorelaxation response of aortic rings [17]. Therefore, an NO concentration of 1 μM is used to define the characteristic NO concentration EC_{1ma}. EC_{1ma} can be considered the minimum NO concentration in the TM that causes a nearly full (>90%) vasorelaxation of the aorta.

Previous experimental data and theoretical analysis have shown that NO diffusion distance in the parenchymal (extravascular) tissue is regulated by oxygen concentration [10]. Based on the experimentally measured oxygen dependent NO diffusion fluxes and mathematical models, this study demonstrates that the NO effective diffusion distance in the aortic wall is also significantly regulated by oxygen concentration (Fig. 5).

These results indicate that the regulation of NO effective distance by oxygen concentration occurs not only in the extravascular tissue [10] but also in the vascular wall. The effective NO diffusion distance has a direct relationship with NO dependent vasodilation in the vascular system. Our results suggest that a reduced oxygen concentration will significantly increase the effective NO diffusion distance and cause vasodilation. This is consistent with a large body of experimental evidence demonstrating that hypoxia increases the NO dependent vasodilation in arteries and arterioles [26–29].

Under low oxygen concentration, or hypoxia, NO generation from other non NOS sources increases [30–32]. This rise in NO generation at low oxygen concentration is important for dilating resistance arteries and increasing blood flow to provide more oxygen to the hypoxic tissue, whereas the reduced NO consumption rate at low oxygen concentrations will further enhance the bioavailability of both NOS and non NOS generated NO by extending the effective NO diffusion distance. Thus, it is likely that NO dependent hypoxic vasodilation results from the cooperation of increased NO generation rate and reduced NO consumption rate.

The identity of the main species responsible for NO catabolism in the vascular wall remains unclear. Although the reaction of NO with Hb and myoglobin (Mb) is very rapid, the two proteins are unlikely to be related to vascular NO consumption because Hb mainly exists in RBCs and Mb is mainly in red muscle such as cardiac and type I skeletal muscle. Superoxide may be a candidate for vascular consumption of NO because the reaction rate of superoxide with NO is ~2 orders of magnitude greater than that with Hb or with Mb, and because superoxide can be generated from a number of proteins, including xanthine oxidase and NADPH oxidase, and mitochondria in tissues, including the vascular wall. However, the existence of potent antioxidant systems in the intracellular and extracellular space may greatly limit the overall effect of superoxide on NO catabolism. Experimental data show that NO consumption by cells is not related to the reduction or oxidation of a cellular component [10], implying that superoxide may not be the main species responsible for the cellular NO consumption because superoxide formation needs electrons from a reductant (oxidation of the reductant). Furthermore, in additional experiments, we observed that the rate of vascular NO consumption is reduced by only a few percent in the presence of 600 μM tempol (a SOD mimetic; data not shown). Therefore, superoxide does not seem to be the main species responsible for removing NO from the vascular wall under normal physiological conditions, although it does have some contribution to vascular NO consumption. In disease settings associated with inflammation and oxidative stress, such as ischemia reperfusion, atherosclerosis, and hypertension, superoxide mediated NO degradation would be expected to be of greater importance [33–37].

In recent years, progress has been made in the search to identify the species and mechanisms responsible for vascular NO consumption. It has been reported that cytochrome *c* oxidase in the oxidized state inactivates NO at a significantly higher rate than the same protein in the reduced state [15]. When oxygen concentration decreases from 70 to 0 μM, cytochrome *c* oxidase changes its redox state from oxidized to reduced. In this way, NO concentration in hypoxic tissues will increase because the NO consumption rate is reduced as the oxidized cytochrome *c* oxidase is converted to its reduced form. The increased NO concentration stimulates sGC, leading to vascular dilatation. Very recently, it was reported that cytoglobin, a newly discovered hexacoordinated globin, contributes to cell mediated NO dioxygenation and it was suggested that cytoglobin may represent an important oxygen dependent NO sink in the vascular wall [16]. Overall our results and those in the literature suggest that metal centers of certain specific proteins serve as the major mediators of vascular NO consumption under normal physiological conditions, whereas superoxide mediated degradation may have a greater role in disease pathophysiology associated with inflammation and oxidative stress.

In conclusion, we demonstrate that the NO concentration distribution in vessels changes with oxygen concentration, with greatly increased NO diffusion distance at low oxygen levels compared to that at high oxygen levels. These results suggest that oxygen dependent NO consumption can have an important role in dilating blood vessels during hypoxia by increasing the effective NO diffusion distance.

Acknowledgments

This work was supported by National Institutes of Health Grants HL063744, HL065608, and HL38324.

References

[1] Lancaster Jr., J. R. Simulation of the diffusion and reaction of endogenously produced nitric oxide. *Proc. Natl. Acad. Sci. USA* **91:**8137–8141; 1994.
[2] Cable, R. G. Hemoglobin determination in blood donors. *Transfus. Med. Rev.* **9:** 131–144; 1995.
[3] Liu, X.; Miller, M. J.; Joshi, M. S.; Sadowska-Krowicka, H.; Clark, D. A.; Lancaster Jr., J. R. Diffusion-limited reaction of free nitric oxide with erythrocytes. *J. Biol. Chem.* **273:**18709–18713; 1998.
[4] Vaughn, M. W.; Huang, K. T.; Kuo, L.; Liao, J. C. Erythrocytes possess an intrinsic barrier to nitric oxide consumption. *J. Biol. Chem.* **275:**2342–2348; 2000.
[5] Tsoukias, N. M.; Popel, A. S. Erythrocyte consumption of nitric oxide in presence and absence of plasma-based hemoglobin. *Am. J. Physiol. Heart Circ. Physiol.* **282:** H2265–H2277; 2002.
[6] Liu, X.; Samouilov, A.; Lancaster Jr., J. R.; Zweier, J. L. Nitric oxide uptake by erythrocytes is primarily limited by extracellular diffusion not membrane resistance. *J. Biol. Chem.* **277:**26194–26199; 2002.
[7] Han, T. H.; Pelling, A.; Jeon, T. J.; Gimzewski, J. K.; Liao, J. C. Erythrocyte nitric oxide transport reduced by a submembrane cytoskeletal barrier. *Biochim. Biophys. Acta* **1723:**135–142; 2005.
[8] Liu, X.; Yan, Q.; Baskerville, K. L.; Zweier, J. L. Estimation of nitric oxide concentration in blood for different rates of generation: evidence that intravascular nitric oxide levels are too low to exert physiological effects. *J. Biol. Chem.* **282:**8831–8836; 2007.
[9] Sakai, H.; Sato, A.; Masuda, K.; Takeoka, S.; Tsuchida, E. Encapsulation of concentrated hemoglobin solution in phospholipid vesicles retards the reaction with NO, but not CO, by intracellular diffusion barrier. *J. Biol. Chem.* **283:**1508–1517; 2008.
[10] Thomas, D. D.; Liu, X.; Kantrow, S. P.; Lancaster Jr., J. R. The biological lifetime of nitric oxide: implications for the perivascular dynamics of NO and O_2. *Proc. Natl. Acad. Sci. USA* **98:**355–360; 2001.

[11] Gardner, P. R.; Martin, L. A.; Hall, D.; Gardner, A. M. Dioxygen-dependent metabolism of nitric oxide in mammalian cells. *Free Radic. Biol. Med.* **31:**191–204; 2001.
[12] Wink, D. A.; Darbyshire, J. F.; Nims, R. W.; Saavedra, J. E.; Ford, P. C. Reactions of the bioregulatory agent nitric oxide in oxygenated aqueous media: determination of the kinetics for oxidation and nitrosation by intermediates generated in the NO/O_2 reaction. *Chem. Res. Toxicol.* **6:**23–27; 1993.
[13] Lewis, R. S.; Deen, W. M. Kinetics of the reaction of nitric oxide with oxygen in aqueous solutions. *Chem. Res. Toxicol.* **7:**568–574; 1994.
[14] Liu, X.; Liu, Q.; Gupta, E.; Zorko, N.; Brownlee, E.; Zweier, J. L. Quantitative measurements of NO reaction kinetics with a Clark-type electrode. *Nitric Oxide* **13:**68–77; 2005.
[15] Palacios-Callender, M.; Hollis, V.; Mitchison, M.; Frakich, N.; Unitt, D.; Moncada, S. Cytochrome c oxidase regulates endogenous nitric oxide availability in respiring cells: a possible explanation for hypoxic vasodilation. *Proc. Natl. Acad. Sci. USA* **104:**18508–18513; 2007.
[16] Halligan, K. E.; Jourd'heuil, F. L.; Jourd'heuil, D. Cytoglobin is expressed in the vasculature and regulates cell respiration and proliferation via nitric oxide dioxygenation. *J. Biol. Chem.* **284:**8539–8547; 2009.
[17] Yan, Q.; Liu, Q.; Zweier, J. L.; Liu, X. Potency of authentic nitric oxide in inducing aortic relaxation. *Pharmacol. Res.* **55:**329–334; 2007.
[18] Liu, X.; Srinivasan, P.; Collard, E.; Grajdeanu, P.; Zweier, J. L.; Friedman, A. Nitric oxide diffusion rate is reduced in the aortic wall. *Biophys. J.* **94:**1880–1889; 2008.
[19] Paul, R. J. Chemical energetics of vascular smooth muscle. In: Bohr, D.R., Somlyuo, A.P., Sparks, H.V. (Eds.), Handbook of Physiology, Vol. II. Waverly Press, Baltimore, pp. 201–235; 1980.
[20] Liu, X.; Cheng, C.; Zorko, N.; Cronin, S.; Chen, Y. R.; Zweier, J. L. Biphasic modulation of vascular nitric oxide catabolism by oxygen. *Am. J. Physiol. Heart Circ. Physiol.* **287:**H2421–H2426; 2004.
[21] Buerk, D. G.; Lamkin-Kennard, K.; Jaron, D. Modeling the influence of superoxide dismutase on superoxide and nitric oxide interactions, including reversible inhibition of oxygen consumption. *Free Radic. Biol. Med.* **34:**1488–1503; 2003.
[22] Lamkin-Kennard, K. A.; Buerk, D. G.; Jaron, D. Interactions between NO and O_2 in the microcirculation: a mathematical analysis. *Microvasc. Res.* **68:**38–50; 2004.
[23] Goldstein, S.; Czapski, G. Kinetics of nitric oxide autoxidation in aqueous solution in the absence and presence of various reductants: the nature of the oxidizing intermediates. *J. Am. Chem. Soc.* **117:**12078–12084; 1995.
[24] Vaughn, M. W.; Kuo, L.; Liao, J. C. Effective diffusion distance of nitric oxide in the microcirculation. *Am. J. Physiol. Heart Circ. Physiol.* **274:**H1705–H1714; 1998.
[25] Chen, K.; Pittman, R. N.; Popel, A. S. Nitric oxide in the vasculature: where does it come from and where does it go? A quantitative perspective. *Antioxid. Redox Signaling* **10:**1185–1198; 2008.
[26] Takehara, Y.; Nakahara, H.; Okada, S.; Yamaoka, K.; Hamazaki, K.; Yamazato, A.; Inoue, M.; Utsumi, K. Oxygen concentration regulates NO-dependent relaxation of aortic smooth muscles. *Free Radic. Res.* **30:**287–294; 1999.
[27] Bauser-Heaton, H. D.; Bohlen, H. G. Cerebral microvascular dilation during hypotension and decreased oxygen tension: a role for nNOS. *Am. J. Physiol. Heart Circ. Physiol.* **293:**H2193–H2201; 2007.
[28] Edmunds, N. J.; Marshall, J. M. The roles of nitric oxide in dilating proximal and terminal arterioles of skeletal muscle during systemic hypoxia. *J. Vasc. Res.* **40:** 68–76; 2003.
[29] Van Mil, A. H.; Spilt, A.; Van Buchem, M. A.; Bollen, E. L.; Teppema, L.; Westendorp, R. G.; Blauw, G. J. Nitric oxide mediates hypoxia-induced cerebral vasodilation in humans. *J. Appl. Physiol.* **92:**962–966; 2002.
[30] Stamler, J. S.; Jia, L.; Eu, J. P.; McMahon, T. J.; Demchenko, I. T.; Bonaventura, J.; Gernert, K.; Piantadosi, C. A. Blood flow regulation by S-nitrosohemoglobin in the physiological oxygen gradient. *Science* **276:**2034–2037; 1997.
[31] Cosby, K.; Partovi, K. S.; Crawford, J. H.; Patel, R. P.; Reiter, C. D.; Martyr, S.; Yang, B. K.; Waclawiw, M. A.; Zalos, G.; Xu, X.; Huang, K. T.; Shields, H.; Kim-Shapiro, D. B.; Schechter, A. N.; Cannon 3rd, R. O.; Gladwin, M. T. Nitrite reduction to nitric oxide by deoxyhemoglobin vasodilates the human circulation. *Nat. Med.* **9:**1498–1505; 2003.
[32] Li, H.; Samouilov, A.; Liu, X.; Zweier, J. L. Characterization of the effects of oxygen on xanthine oxidase-mediated nitric oxide formation. *J. Biol. Chem.* **279:** 16939–16946; 2004.
[33] Zweier, J. L.; Kuppusamy, P.; Williams, R.; Rayburn, B. K.; Smith, D.; Weisfeldt, M. L.; Flaherty, J. T. Measurement and characterization of postischemic free radical generation in the isolated perfused heart. *J. Biol. Chem.* **264:**18890–18895; 1989.
[34] Zweier, J. L.; Talukder, M. A. The role of oxidants and free radicals in reperfusion injury. *Cardiovasc. Res.* **70:**181–190; 2006.
[35] Harrison, D. G.; Cai, H.; Landmesser, U.; Griendling, K. K. Interactions of angiotensin II with NAD(P)H oxidase, oxidant stress and cardiovascular disease. *J. Renin Angiotensin Aldosterone Syst.* **4:**51–61; 2003.
[36] Touyz, R. M. Reactive oxygen species, vascular oxidative stress, and redox signaling in hypertension: what is the clinical significance? *Hypertension* **44:** 248–252; 2004.
[37] Nedeljkovic, Z. S.; Gokce, N.; Loscalzo, J. Mechanisms of oxidative stress and vascular dysfunction. *Postgrad. Med. J.* **79:**195–199; 2003.